



**US Army Corps
of Engineers®**
Engineer Research and
Development Center

Tensar International Corporation

Full-Scale Accelerated Pavement Tests

Geogrid Reinforcement of Thin Asphalt Pavements

Phase 1 Interim Report

Sarah R. Jersey, and Jeb S. Tingle

February 2010



Introduction

Objective and scope of investigation

This investigation served two primary purposes, (1) obtaining pavement response data, and (2) quantifying the benefits of geogrid reinforcement at the base-subgrade interface of an asphalt-surfaced pavement structure. As a part of the study, mechanistic response data were obtained from the various pavement sections, including unreinforced and geogrid reinforced test items, for validation of performance models and design models developed by Tensar International Corporation for their geogrid products. Phase 1 of the study was designed to provide a validation of performance behavior for Tensar TriAx geogrid relative to two unreinforced control sections, and can serve as validation of design protocols developed and used by Tensar International Corporation for pavement design with TriAx geogrid. In addition, two additional prototype geogrids were tested during this study. To accomplish this, a full-scale test section was constructed containing five different test items. Each test item represented a different pavement structure. Each item was trafficked using simulated truck traffic applied via the ERDC Heavy Vehicle Simulator (HVS).

Test Plan and Test Section Layout

The test section consisted of five different test items. Each test item was 50 ft long and 8 ft wide. A plan view of the test section is shown in Figure 1. The test items were constructed simultaneously and with extensive quality control measures to minimize variability between and/or within test items.

The structural design of the test section was developed following the guidelines set forth in the AASHTO 1993 design guide (AASHTO 1993). The design was developed using the tools and tables provided in the 2nd Edition of Pavement Analysis and Design (Huang, 2004). The structural design of the pavement is based upon a representative structural number of 2.0 for an unreinforced low-volume pavement.

These calculations assumed a reliability for low-volume roads of 50%, and a change in serviceability of 2.2. The low reliability represented a 50% likelihood of failure at the design load level, which is desirable when designing a test section. It is critical that the pavement design not be conservative to ensure pavement failure within a reasonable number of load cycles, which provides useful performance data. A change in serviceability of 2.2 assumed an initial serviceability of 4.2, consistent with initial conditions for a flexible pavement, and a terminal serviceability of 2.0, as suggested by AASHTO for lower volume roadways.

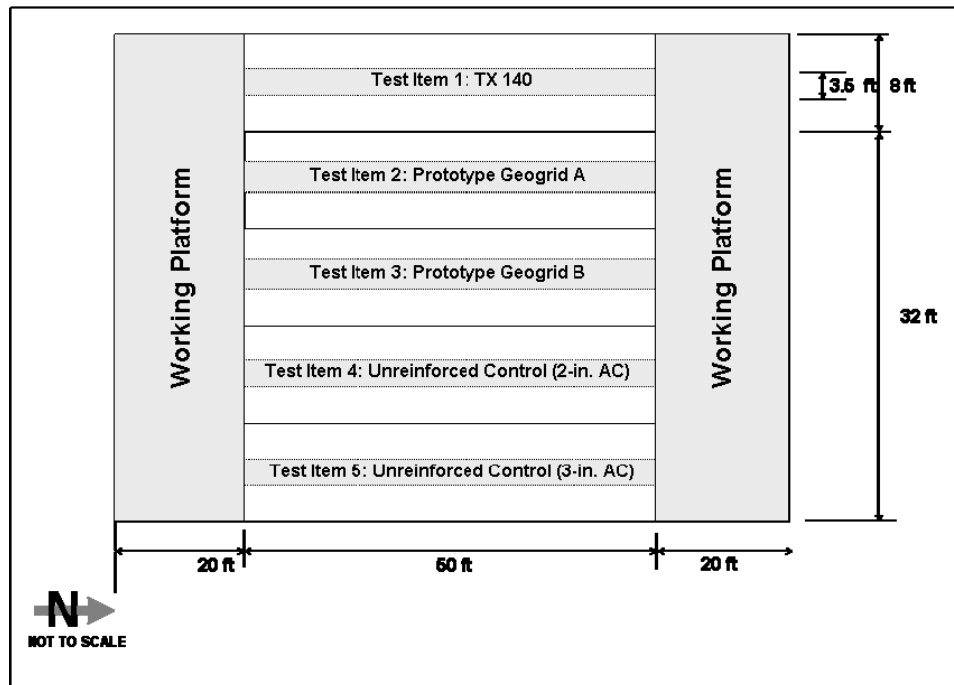


Figure 1. Plan view of test section.

This pavement was designed for a traffic level of 125 vehicles per day, based upon traffic levels typical of low-volume roads. A truck factor of 0.30 was applied (Huang, 2004). This corresponds to a typical truck factor on a rural collector road. It was assumed that trucks constituted 15% of the total traffic mix, consistent with a Category III roadway (TM 5-82-5). Based on these assumptions the design traffic over a 20-year performance period was 41,000 ESALS for the 3 CBR subgrade condition.

Resilient moduli were estimated using the design CBR of the base and subgrade. These conditions were used to develop the representative structural number of 2.0. At the projected traffic level, a minimum asphalt thickness of 2 inches is required. A structural coefficient of 0.44 was assigned to the asphalt layer while a structural coefficient of 0.14 was assigned to the granular base. These values are consistent with the structural coefficients from the AASHO Road Test. Based on these values, a minimum base thickness of 7.8 inches was computed. The final pavement structure was constructed with a design base course thickness of 8 in. to facilitate construction.

A profile view of the pavement structural design is shown in Figure 2. Each test item was constructed with 28 in. of high-plasticity clay as the subgrade material. The subgrade was overlain with an 8-in. thick base course consisting of crushed limestone. The limestone was covered with a thin asphalt concrete surface course. Item 1 was constructed with Tensar's TX140 geogrid product at the base-subgrade interface while Items 2 and 3 were constructed with prototype geogrids at the base-subgrade interface.

The geogrid-reinforced items (1, 2, and 3) were surfaced with a 2-in. thick asphalt concrete surface layer. Items 4 and 5 were unreinforced control items; representing traditional thin highway pavement structures. Item 4 was constructed with a 2-in. thick asphalt concrete surface layer while Item 5 was constructed with a 3-in. thick asphalt concrete surface layer. The test items were constructed simultaneously at the Hangar No. 4 pavement test facility at ERDC's Vicksburg, MS location. The open-ended hangar minimizes the detrimental effect of rainfall to the test pavements. A drain was installed along the north end of the test section to prevent moisture intrusion due to potential drainage from outside Hangar 4.

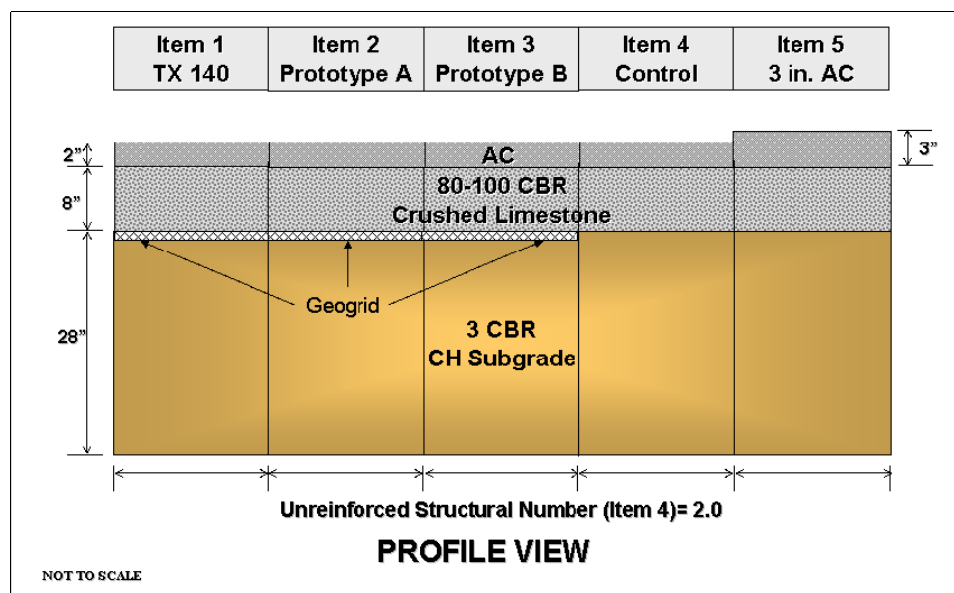


Figure 2. Profile view of test section.

Material Characterization

Materials used during construction of the test section are described in this section. Subgrade, base, and asphalt concrete materials underwent a suite of laboratory characterization tests prior to construction of the test section. The results of these tests are summarized in this section.

Subgrade

The subgrade was constructed using locally available clay, known as Vicksburg Buckshot Clay. Figure 3 shows the gradation of the Buckshot Clay used in this test item. The soil is composed of 98% fines passing the #200 sieve. The liquid limit, plastic limit, and plastic index were determined to be 83, 29, and 54, respectively following the procedures described in ASTM C 856-02-07. The soil classifies as a high-plasticity clay (CH)

in the Unified Soil Classification System (USCS) and an A-7-6(63) according the AASHTO procedure.

When processed to a uniform moisture and density condition, the CH material produces a uniform strength profile. The moisture capacity and reduced permeability of the material lead to a relationship between the moisture content of the CH and the resulting strength, as shown in Figure 3. Based on this relationship, a moisture content of approximately 41.0% is required to obtain the 3 CBR strength required for the subgrade.

Modified Proctor tests were performed in accordance with ASTM D 1557-07--07, Method A Modified. The results of this test are shown in Figure 4. At the target moisture content of 41.0%, the maximum dry density was 78.4 pcf.

Base course

The base course was constructed using crushed limestone. This material is considered a typical high quality aggregate for construction in Mississippi highway pavements. Figure 6 shows the gradation of this aggregate. The soil was composed of 61% gravel, 32% sand, and 7% fines passing the #200 sieve with nonplastic fines. The coefficients of curvature (C_c), and uniformity (C_u) were 3.55 and 49.33, respectively. The soil is classified as a poorly graded silty gravel (GP-GM) in the Unified Soil Classification System (USCS) and A-1-a according the AASHTO procedure.

Modified proctor tests were performed in accordance with ASTM D 1557-07-07, Method C Modified. The results of this test are shown in Figure 7. At the optimum moisture content of 4.3%, the maximum dry density is 148.9 pcf.

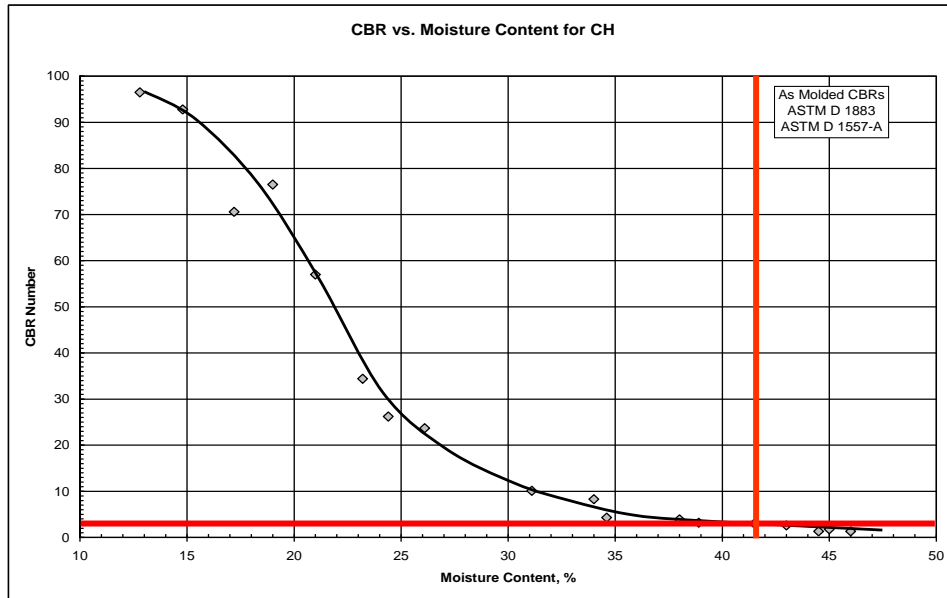


Figure 4. Historical moisture content - strength relationship for Vicksburg Buckshot Clay.

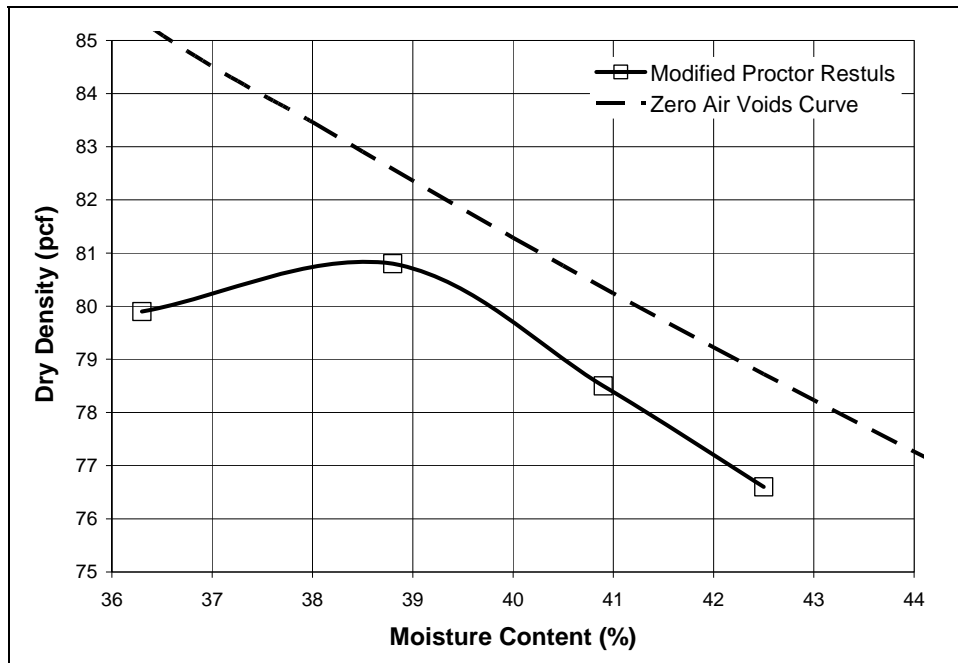


Figure 5. Moisture-density results from modified proctor testing of subgrade materials.

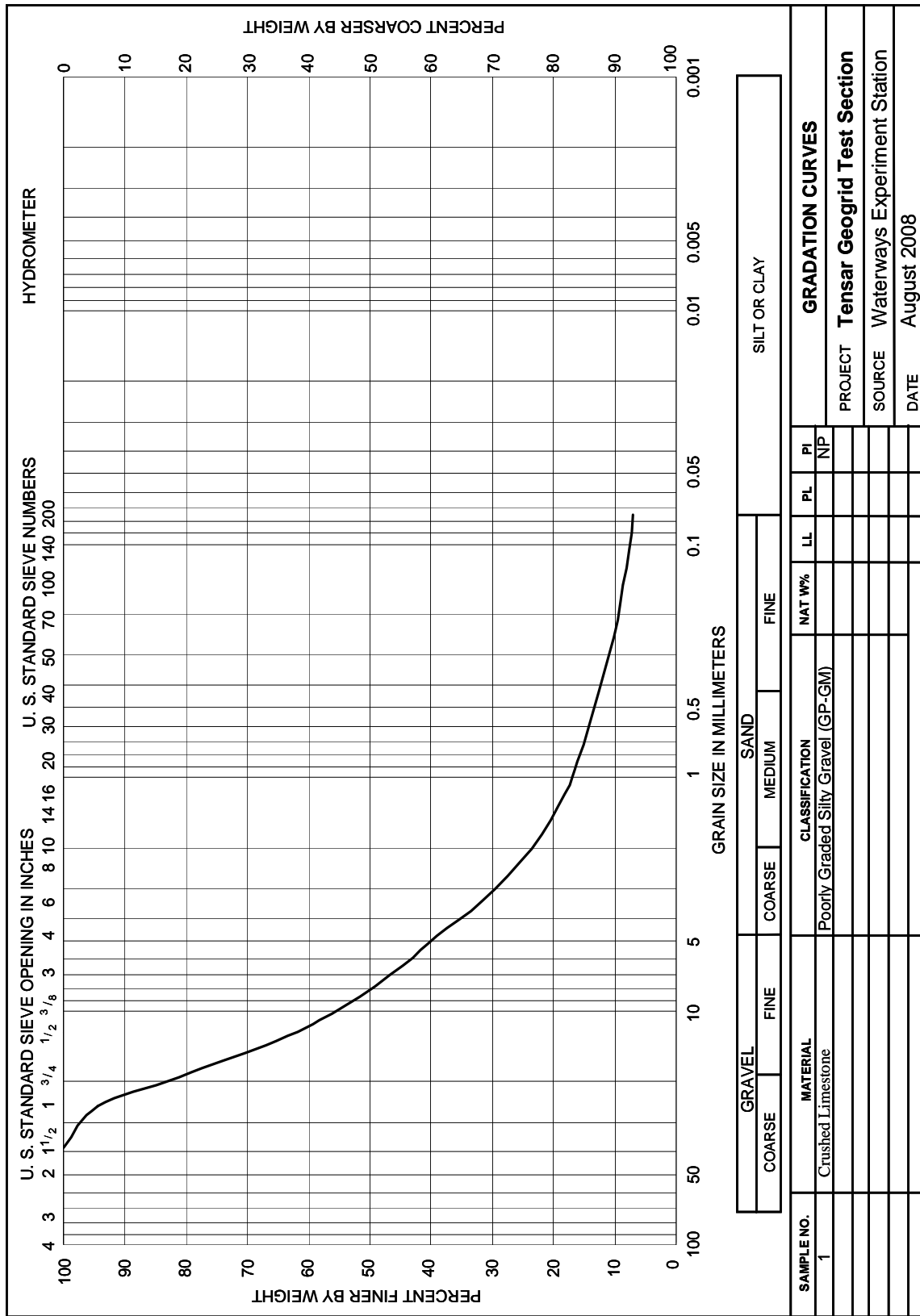


Figure 6. Crushed Limestone base course gradation.

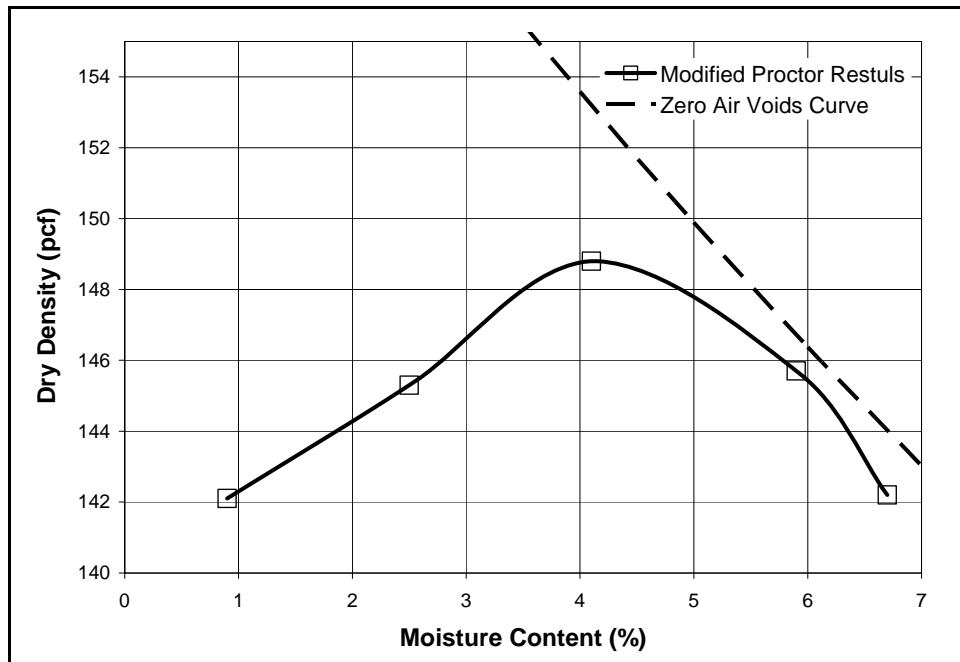


Figure 7. Moisture-density results from modified proctor testing of base course materials.

Asphalt

The asphalt concrete used as a surface material in this test section was selected as representative of a highway mix for Mississippi. Laboratory tests were performed to characterize the asphalt. Aggregate gradation was measured using the wet sieve method (AASHTO T 27). The gradation is summarized in Table 1. Table 2 presents the results of the Marshall mix design tests. The recommended values for Marshall mix design for a medium volume road (10,000-1,000,000 ESALS) are also presented in Table 3 (Asphalt Institute, 1979). The mix used in this test meets the Asphalt Institute guidance.

Table 1. Aggregate gradation for asphalt concrete blend.

US Standard Sieve Size	Diameter (in.)	Percent Finer
1 in.	1.00	100.0
3/4 in.	0.75	99.3
1/2 in.	0.50	99.0
3/8 in.	0.375	94.6
No. 4	0.187	59.2
No. 8	0.0937	34.4
No. 16	0.0394	24.2
No. 30	0.0234	19.0
No. 50	0.0117	11.1
No. 100	0.0049	7.8
No. 200	0.0029	5.6

Table 2. Marshall mix design results for asphalt concrete.

Test	Result
Marshall Stability (lb) AASHTO T 245	3359
Marshall Flow (0.01 in) AASHTO T 245	12.7
Tensile Strength Ratio (%)	104
Specific Gravity AASHTO T 209	2.425
Asphalt Content (%)	4.87
Percent Air Voids (%) AASHTO T 269	4.48

Table 3. Recommended Mix Design for 10,000-1,000,000 ESALS (Asphalt Institute, 1997).

Test	Maximum	Minimum
Stability (lb)	750	
Flow (0.01 in.)	8	18
Air Voids (%)	3	5

Instrumentation

Sensors were placed in the asphalt concrete, the aggregate base, the subgrade, and on the geogrid surface to obtain measures of pavement response under traffic loading. Dynamic sensors included earth pressure cells (EPCs), single-depth deflectometers (SDDs), asphalt strain gauges (ASGs), and geogrid strain gauges (GGs). Figure 8 shows the sensor locations in a profile view. All instruments were centered horizontally within the traffic lane.

Environmental sensors were placed in the subgrade to monitor environmental parameters as shown in Figure 9. These sensors were placed to provide measures of changes in soil moisture (volumetric), temperature, and pore pressure in the subgrade. Additionally, sensors were placed in the asphalt concrete and in the HVS chamber to monitor the temperature at these locations during traffic testing.

All instrumentation was placed after the respective pavement layers were constructed, except the geogrid strain gauges and the asphalt temperature gauges. The geogrid strain gauges were attached to the geogrid prior to installation of the geogrid at the subgrade surface while the asphalt temperature gauges were installed after pavement construction, prior to traffic testing.

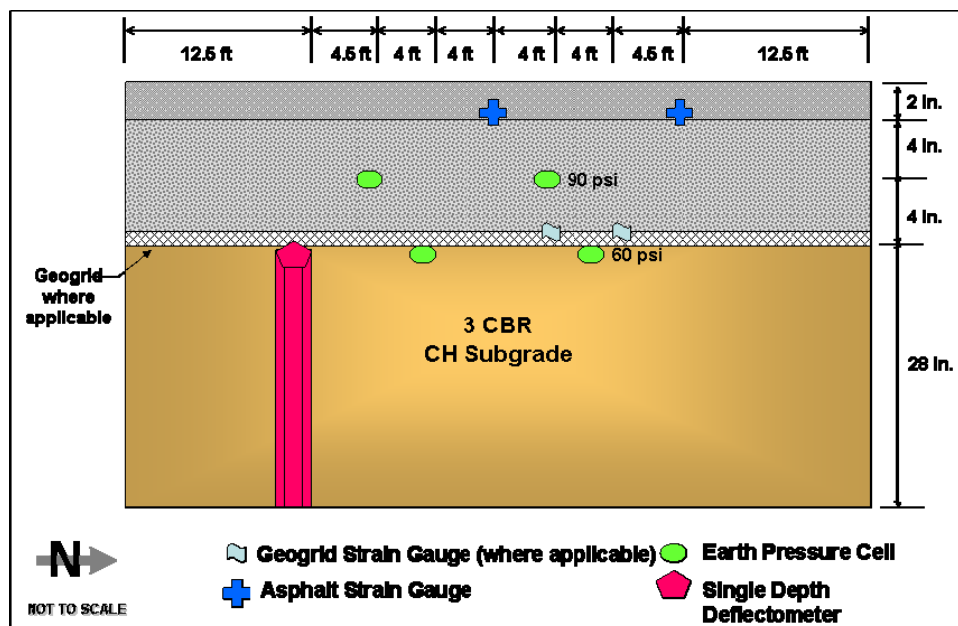


Figure 8. Dynamic sensors, profile view.

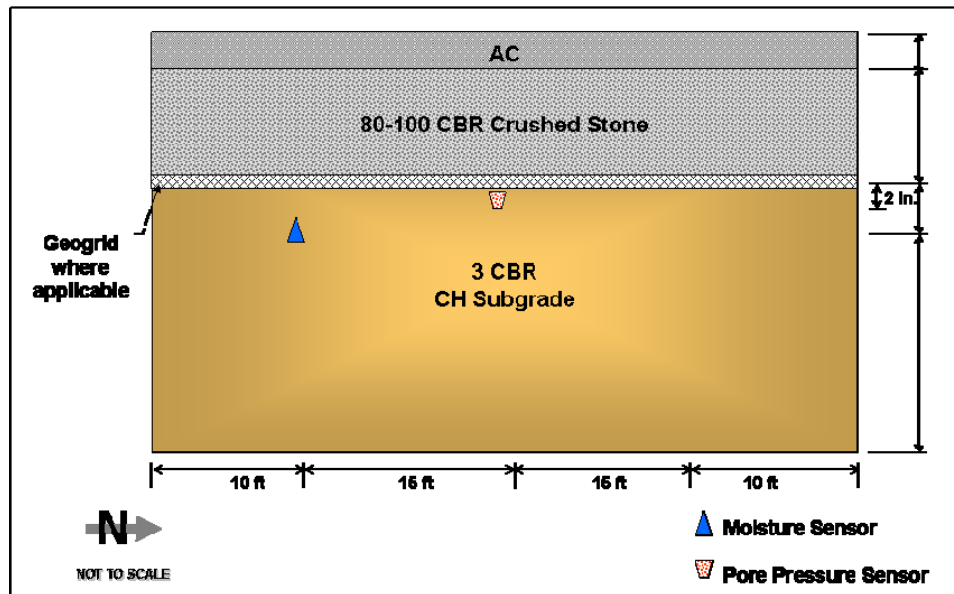


Figure 9. Environmental sensors, profile view.

Earth Pressure Cells

Vertical stresses were measured using a series of 9-in. diameter earth pressure cells (EPCs). Observations from EPCs provide a quantitative measure of the vertical distribution of the stresses in the various test items. The geogrid reinforced pavements should distribute the tire load over a broader area than the unreinforced control due to the increased stiffness of the base course.

Two Geokon Model 3500 EPCs with a maximum pressure range of 58 psi were placed two inches below the base-subgrade interface in each test item. A second pair of Model 3500 EPCs was placed in the center of the base. The EPCs in the base have a maximum pressure range of 87 psi. The maximum pressure ranges required for the EPCs were specified based on linear elastic analyses of the predicted stresses at these depths in the pavement system. Photo 1 shows the installation of an EPC just below the base-subgrade interface.



Photo 1. Centering EPC under stringline at desired station.

Asphalt Strain Gauges

The strain at the bottom of the asphalt surface course was measured using asphalt strain gauges (ASGs). The tensile strain at the bottom of an asphalt layer provides a measure of the pavement response. Increases in permanent, or plastic, strain lead to pavement failure. The strain at this location can be used to estimate the fatigue life of the asphalt surface layer of the pavement.

Two pairs of CTL Model ASG-152 ASGs with a range of 1500 microstrain were placed in each test item. Each pair consisted of an ASG located in the center of the traffic lane aligned such that it measured longitudinal strain and a second ASG aligned in the center of the traffic lane to measure transverse strain at the bottom of the AC layer. The transverse gauge was centered at the station shown in Figure 9. The longitudinal gauge was centered approximately 2 ft north of the transverse gauge. The layout of these gauges prior to asphalt paving is shown in Photo 2.



Photo 2. Asphalt strain gauges were covered with cold patch prior to paving operations

Geogrid Strain Gauges

A number of strain gauges were placed directly on the geogrids prior to installation of the geogrids and the base course. These strain gauges provide a means of measuring the level of strain along a rib of the geogrid.

One of the primary mechanisms by which it is suspected that geogrid reinforcement works is through lateral restraint of the base course. In order for the geogrid to properly perform, a certain amount of strain must be mobilized, essentially locking the geogrid and aggregate into a stiff sublayer at the bottom of the base course. Strain measurements along the geogrid provide a means of quantifying the geogrid mobilization.

Strain gauges were placed on the geogrid products in two locations per test item. Gauges were installed by Ables Electronics, Inc. Vichay Micro-Measurements gauges (either EP-08-500GB-120 and EP-08-230DS-120, depending on the geogrid dimensions) were installed on the geogrids. Installation consisted of carefully attaching the gauge to the grid and trimming it to size. The strain gauges were then covered with Aqua-Seal to prevent moisture damage. Finally, an epoxy coat was applied to provide additional protection to the strain gauges. Photo 3 shows the installed gauges.

Gauges were applied to the individual ribs (in between the nodes of a single rib) of the geogrids. Wiring was laid in a trench in the subgrade below the geogrid to prevent damage during base course installation. The wooden supports were removed and the

strain gauges were covered with sand to prevent damage due to large aggregates during base course construction (Photo 4).



Photo 3. Geogrid strain gauges on TriAx geogrid product prior to placing epoxy protective layer.



Photo 4. Gauges were covered with sand to prevent damage during base course installation.

Single-Depth Deflectometers

Due to the thin asphalt surface and the relatively low subgrade strength, it is expected that pavement failures during this test will result from subgrade failure (rutting) rather than due to fatigue failure of the asphalt layer. Quantification of the displacement of the subgrade surface can validate the failure mechanism. Measurements of deformations in the subgrade can also be used to quantify the reinforcing benefits of a geogrid. The reductions in vertical stresses at the subgrade are also reflected in the deformation. The geogrid-reinforced pavement should show lower deflections than the unreinforced pavement at a given traffic level.

Vertical deflections in the subgrade were measured using single-depth deflectometers (SDDs). One SDD was placed at the south end of each test item. The SDD was placed such that the shaft was anchored at a depth of 9 ft. A linear velocity displacement transducer (LVDT) with a 1-in. range was placed in the housing such that it was in contact with both the anchor rod and the surface plate (Photo 5). Thus, the LVDT measured movement of the plate 2 inches below the base-subgrade interface relative to the control point located at a depth of 9 feet.



Photo 5. SDD housing prior to placement of LVDT.

Pavement Characterization

A series of tests were performed to characterize the as constructed properties of the pavement materials. During construction, in-field California Bearing Ratio (CBR) values, dry density, and moisture content were obtained for each pavement layer. In-field CBR values were obtained following the standards set forth in ASTM D4429-04 while density and moisture content were obtained following ASTM D 3017-04. These values provide a means of assessing the uniformity of the constructed layers as well as the comparative value of the various pavement layers. The as-built subgrade properties are summarized in Table 4 while the as-built base course properties are summarized in Table 5. The variability shown during construction of these pavements was fairly low for geomaterials.

Table 4 Summary of as-built moisture, density, and strength properties of CH subgrade.

	Item 1	Item 2	Item 3	Item 4	Item 5
Treatment	TX 140	GGA	GGB	Control	3 in. AC
Wet Density (pcf)	113.8	113.8	113.8	114.0	112.9
Dry Density (pcf)	83.6	83.3	83.8	83.5	83.0
Moisture (%)	36.1	36.3	36.2	36.1	36.2
Oven-Dried Moisture (%)	37.0	38.2	38.2	37.9	38.9
CBR (%)	3.1	3.0	3.1	2.9	2.8
In situ vane shear (psi)	15.2	16.1	15.5	15.5	15.9

Table 5. Summary of as-built moisture, density, and strength properties of the crushed limestone base course.

	Item 1	Item 2	Item 3	Item 4	Item 5
Treatment	TX 140	GGA	GGB	Control	3 in. AC
Wey Density (pcf)	153.2	152.7	154.7	153.8	154.6
Dry Density (pcf)	148.8	148.5	150.5	149.7	150.1
Moisture (%)	2.9	2.8	2.8	2.7	3.0
Oven-Dried Moisture (%)	2.3	1.8	2.0	2.1	1.4
CBR Strength (%)	90.5	100+	100+	100+	100+
Thickness (in.)	7.42	7.97	7.88	8.09	7.90

Dynamic Cone Penetrometer

A series of tests were performed using the Dynamic Cone Penetrometer (DCP) to characterize the strength of the unbound pavement layers. DCP tests were performed after construction of the base and subgrade layers, following the procedures described by

ASTM D 6951-09. Measured values of the DCP index (millimeters of penetration per hammer blow) were converted to CBR strength using the relationship developed by Webster et al. (1992, 1994). Figures 10- 14 show the strength profiles obtained after construction of the subgrade in Items 1 through 5. These plots indicate subgrade strengths of 3.5 to 4 CBR. The increase in strength at depths below 12 in. are typical of the high-plasticity clay (CH) used for subgrade construction. This phenomenon, known as stair stepping, reflects adhesion of the clay materials to the DCP rod. In field CBR tests and vane shear tests were also performed after construction of the subgrade. The results of these tests are summarized in Table 4.

Figures 15-19 show the DCP results from tests performed after construction of the base course. These tests show that the high quality limestone base was constructed to a strength of 100 CBR. The transition from base to subgrade was observed around a depth of 8 inches for all three test items.

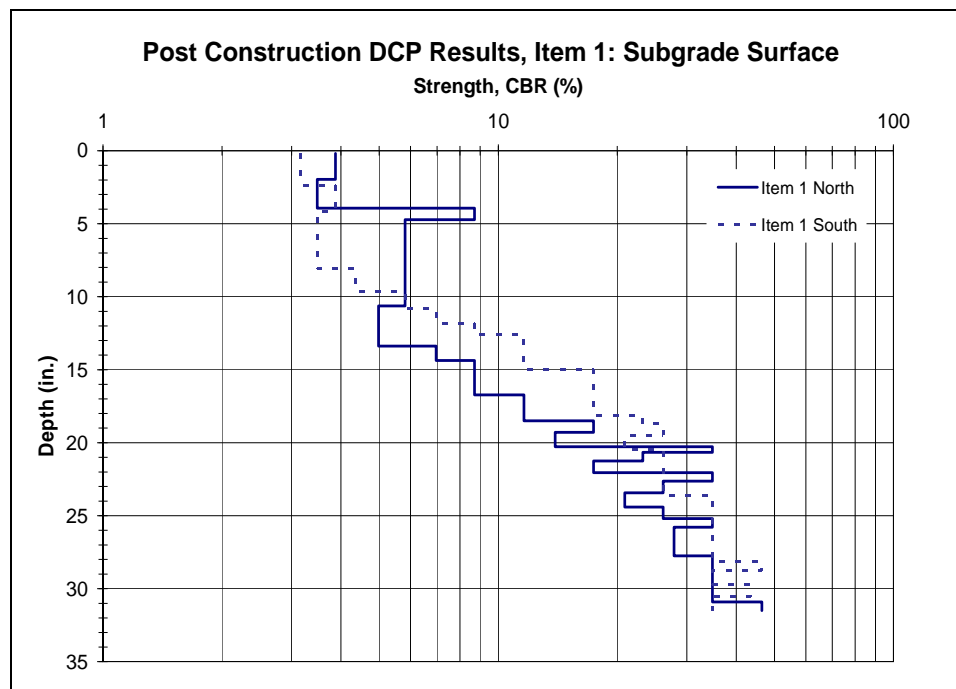


Figure 10. Subgrade strength profile obtained using the DCP, Item 1.

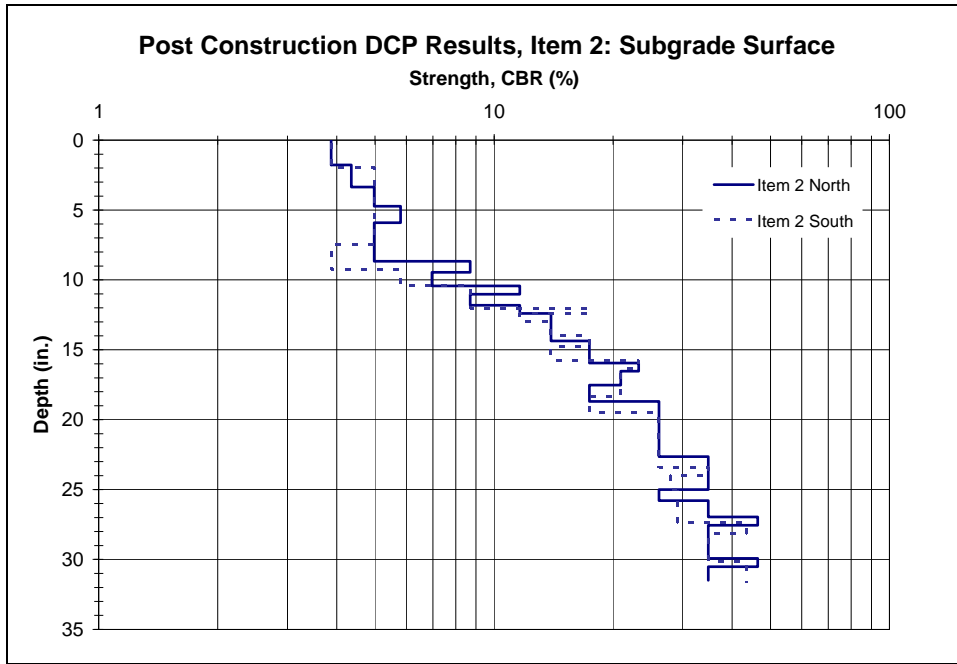


Figure 11. Subgrade strength profile obtained using the DCP, Item 2.

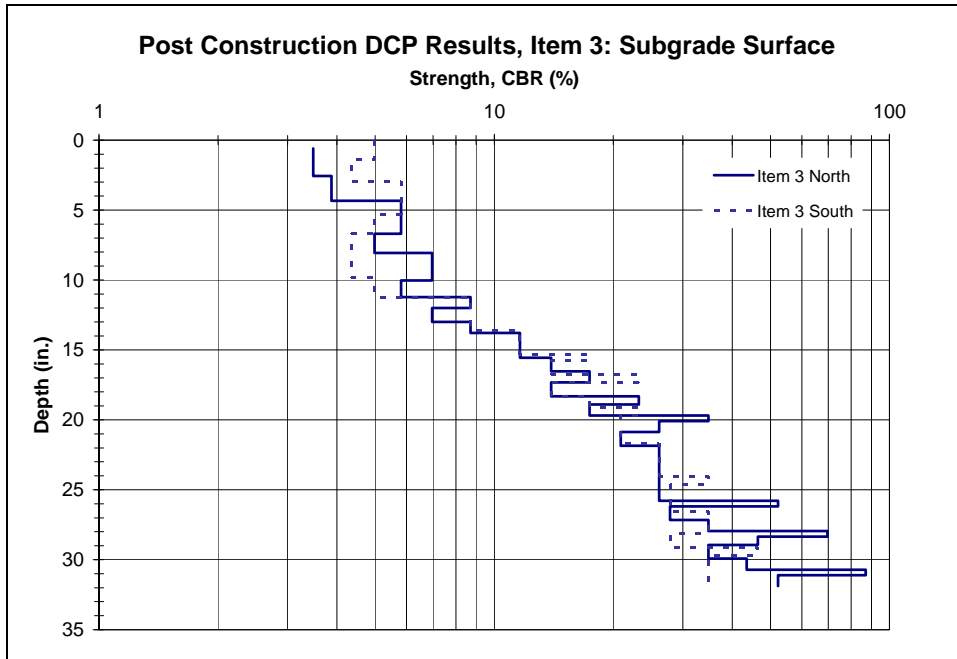


Figure 12. Subgrade strength profile obtained using the DCP, Item 3.

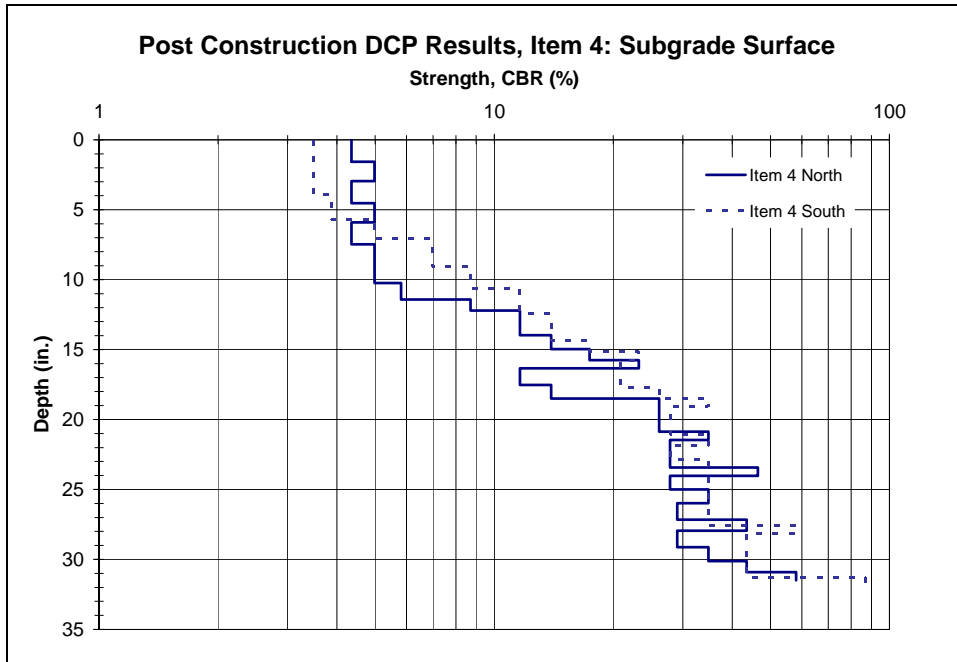


Figure 13. Subgrade strength profile obtained using the DCP, Item 4.

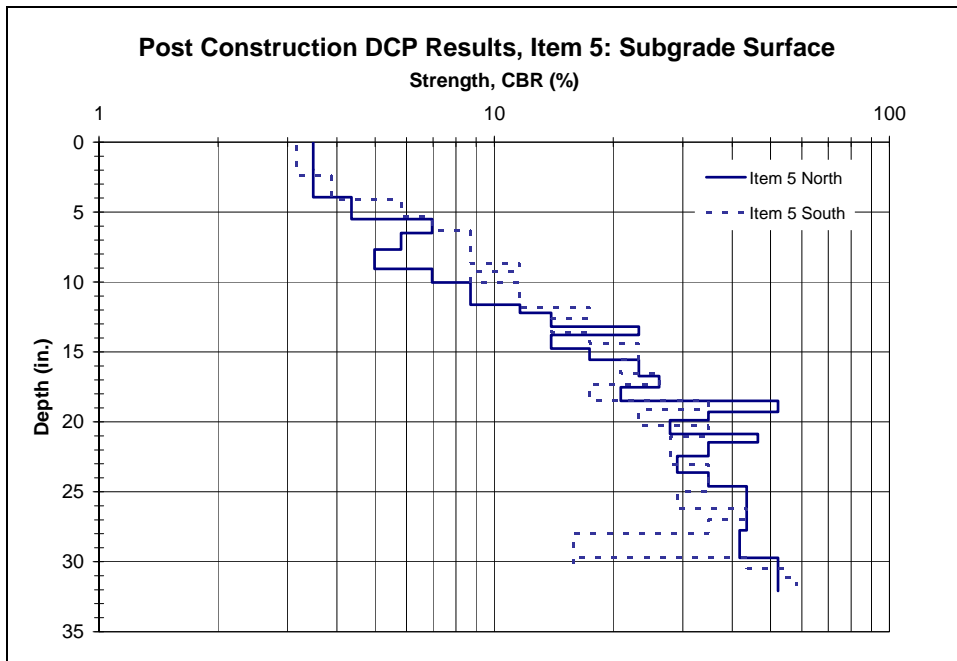


Figure 14. Subgrade strength profile obtained using the DCP, Item 5.

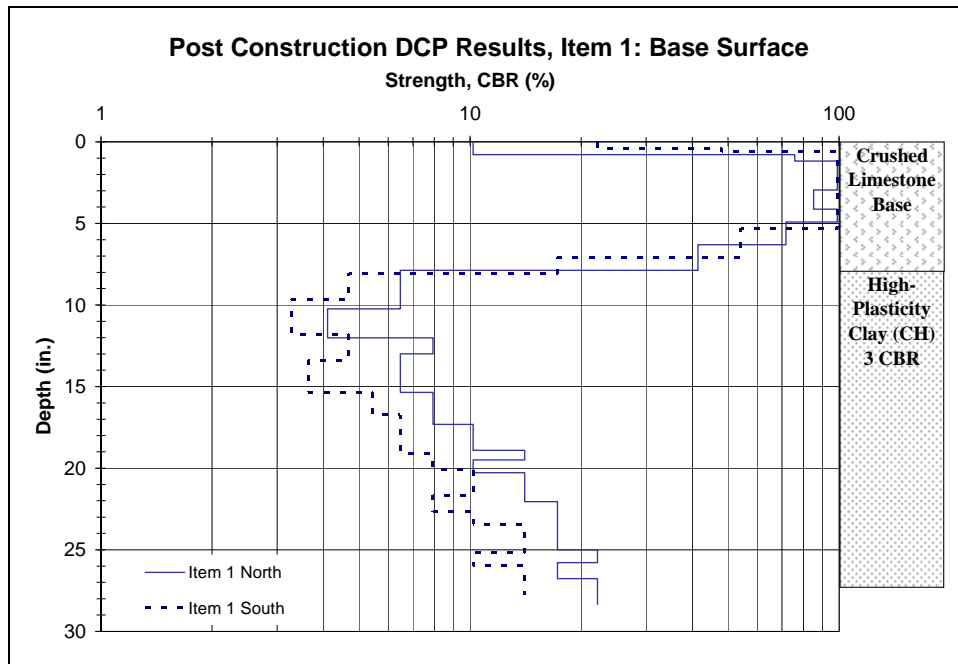


Figure 15. Base and subgrade strength profile obtained using the DCP, Item 1.

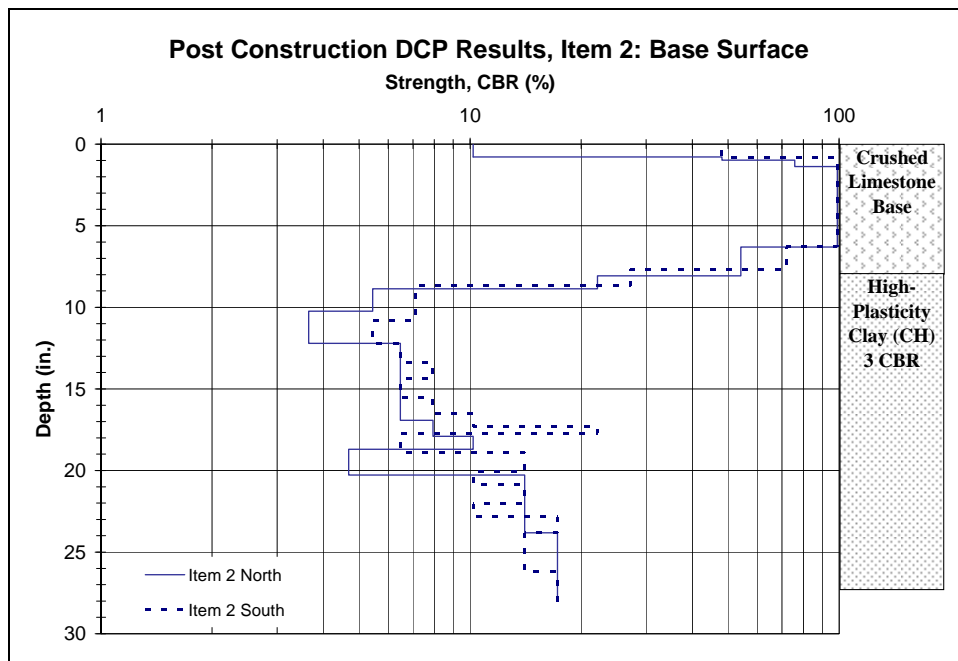


Figure 16. Base and subgrade strength profile obtained using the DCP, Item 2.

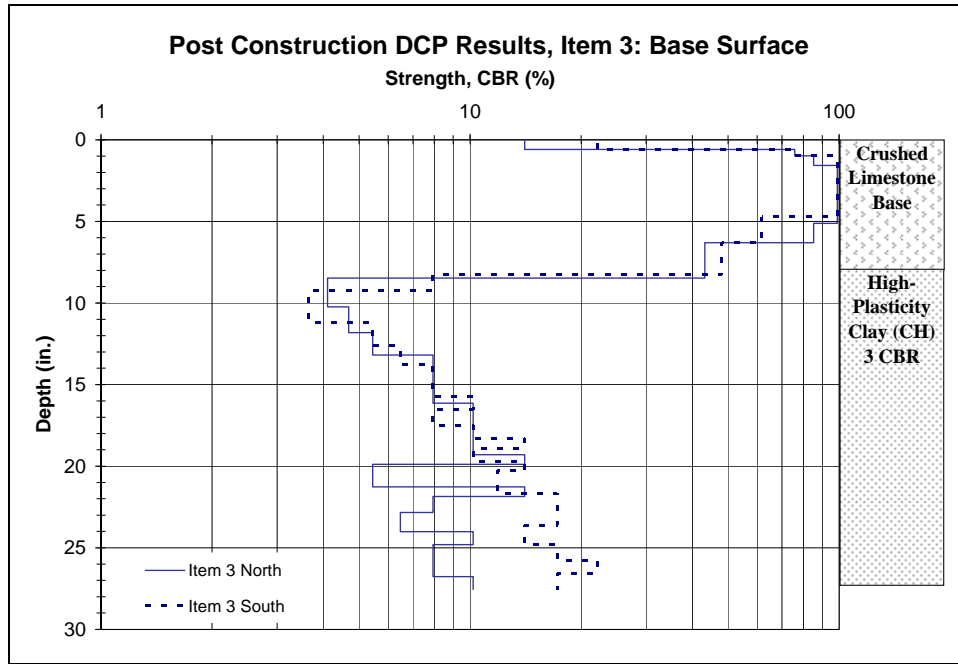


Figure 17. Base and subgrade strength profile obtained using the DCP, Item 3.

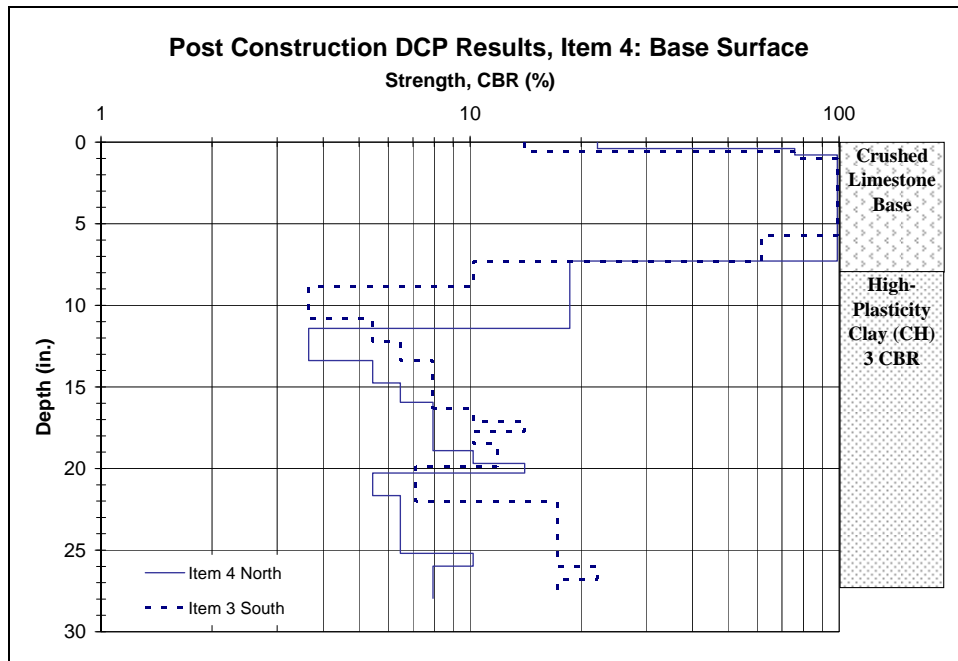


Figure 18. Base and subgrade strength profile obtained using the DCP, Item 4.

erties of the base course (density, strength, and stiffness). In general, the computed ISM values are relatively consistent compared to the variability typically observed in asphalt pavement sections.

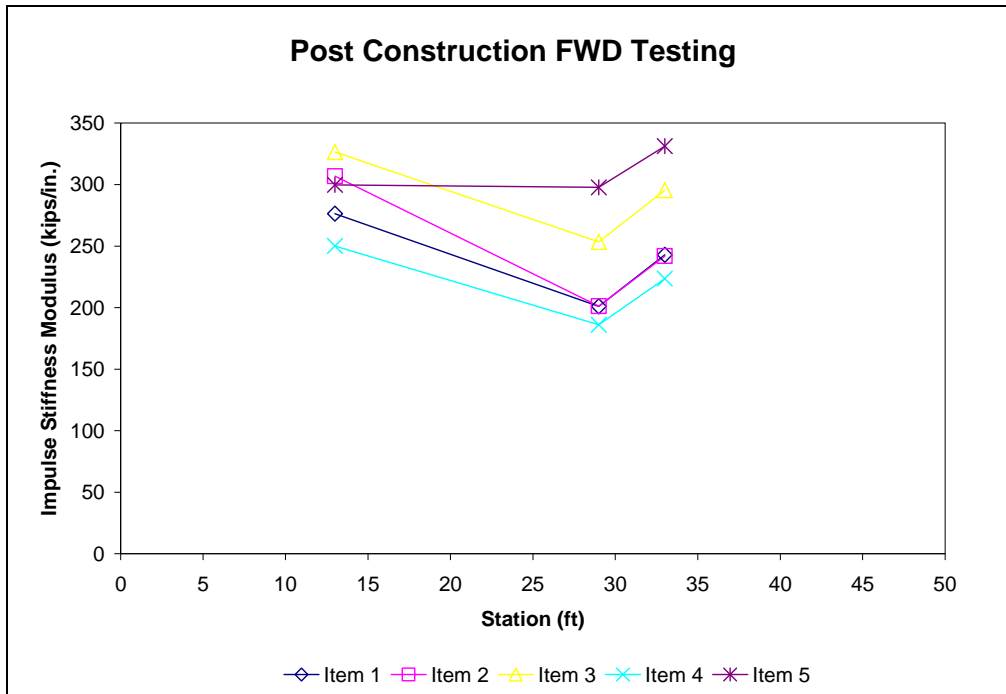


Figure 20. FWD results at selected locations prior to the onset of traffic testing.

Traffic Testing

Traffic testing of the test items was accomplished using the ERDC Heavy Vehicle Simulator (HVS-A). The HVS-A is capable of applying traffic loads between 10,000 and 100,000 lbs. The axle configuration by which the wheel loads are applied to the pavement can be configured to the user's specifications. Variables include the tire, the number of tires, and the applied load. Traffic testing of Item 4 (Control) was accomplished using a dual-wheel single axle loaded to a nominal load of 10,000 lb. This axle is shown in Photo 6. Traffic testing of the remaining test items was accomplished using a dual-wheel tandem axle loaded to a nominal load of 20,000 lb (Photo 7) to accelerate the time required for trafficking. The tandem axle provides double the traffic coverage in a single pass of the load carriage. Adverse effects associated with trafficking using tandem axle rather than the single axle are considered nominal.



Photo 6. Dual-wheel single axle used to traffic Item 4.



Photo 7. Dual-wheel tandem axle used to traffic Items 1, 2 and 5.

The test items were subjected to a uniformly distributed traffic load, as shown in Figure 21. The lateral offset indices refer to 1-in. increments along which the wheel travels longitudinally. Thus, the extent of the lateral wander associated of this traffic pattern is approximately 3 feet. This represents the wander in a typical traffic lane, as observed by Timm and Priest (2005). Traffic loading was applied over a 50-foot length along each

test item. Data collection was performed along the inner 40-ft section of the traffic lane to avoid those stations in the transition zone adjacent to the end of the test lane.

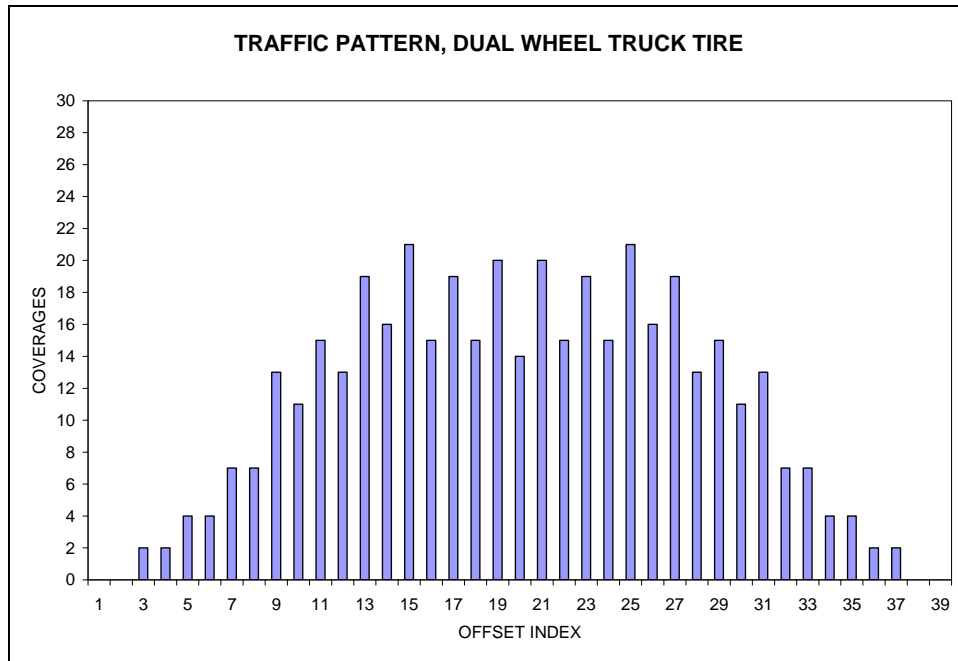


Figure 21. Lateral wander pattern used for traffic application.

At selected traffic intervals, data were collected, including permanent surface deformation and instrumentation response data. The failure criterion for these highway pavements was a 1-in. surface rut, including any upheaval. Each test item was trafficked beyond that level to ensure that adequate pavement response and performance data was obtained.

Preliminary Results

This section includes a summary and discussion of the data collected at the time of this publication, including survey data at the pavement surface, FWD data, and post-traffic forensics for these items tested to date. Initial results for Items 1, 4 and 5 are available at this writing. Trafficking of Items 2 and 3 were not complete at the time of this writing. The full suite of instrumentation and pavement response data has not yet been analyzed.

Surface Deformations

Rut depth is an indicator of pavement performance, particularly in thin pavements such as these where subgrade failure is expected to govern rather than asphalt fatigue. The

measured rut depth is defined as the distance from the bottom of a straight edge placed across the traffic lane to the bottom of the rut trough, including any upheaval along the edges of the traffic lane. In this study, the pavement was considered failed at a rut depth of 1 in. due to the resulting decrease in pavement serviceability. This depth is considered a standard failure level for most accelerated pavement tests on flexible pavement systems. Rutting was measured at five longitudinal locations along each test item (Stations 9, 12.5, 25, 37.5, and 43) at selected traffic intervals throughout traffic testing. Rutting was measured at three transverse locations at each Station, as shown in Figure 22. The average of these values was used to calculate the rut depth at the station. This method provides a means of incorporating the wheel wander into the rutting results.

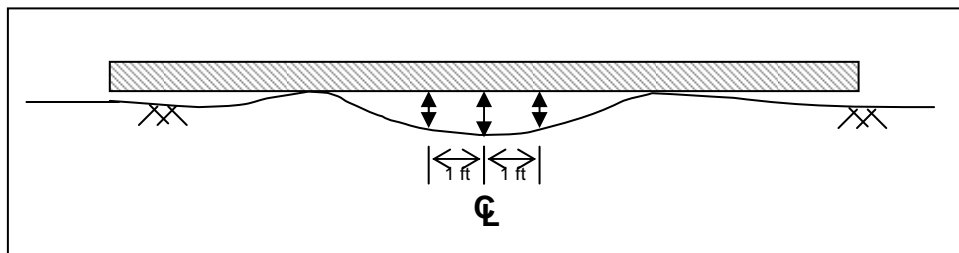


Figure 21. Schematic of rut depth measurement layout.

The average rutting measured at these stations is shown in Figure 23 for Items 1, 4, and 5. As noted previously, results from Items 2 and 3 are not available at the time of this interim report. This figure indicates that the onset of rutting occurred more rapidly in Items 4 and 5 (the unreinforced controls), than in the geogrid reinforced pavement, Item 1. Further, these data indicate that the pavement life of the geogrid reinforced test item exceeded that of the unreinforced test items. It should be noted that trafficking of Item 1 was stopped at 100,000 ESALs due to material contamination from flooding.

In analyses of the test section data, a test item was considered failed when 50% of the test item exceeded a rut depth of 1 in. This is consistent with a reliability of 50% used in the initial pavement design assumptions. The traffic levels at which the various test items failed are summarized in Table 7. This table also includes the traffic levels at which several other pertinent rut levels were exceeded. This analysis is based upon 3 of the 5 stations exceeding the rutting thresholds. These data support the observations discussed previously: the control (Item 4) sustained the least traffic, followed by the thickened asphalt (Item 5), then TX140 (Item 1).

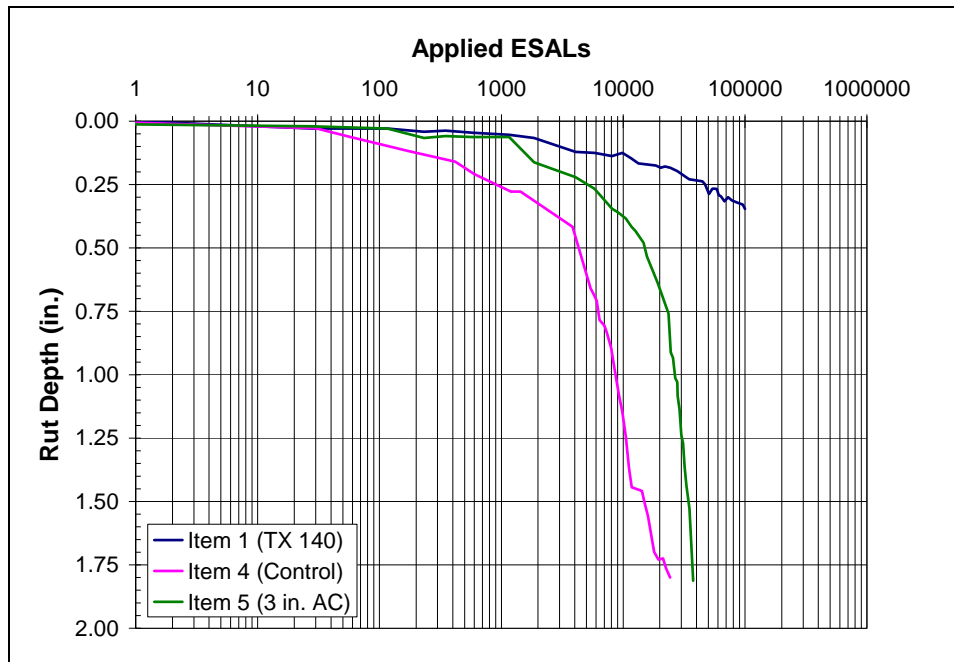


Figure 23. Accumulation of rutting at selected locations

In addition to measurements of rutting at discrete locations, the longitudinal pavement profile was surveyed at a number of traffic levels during testing. These curves provide a more robust method of comparing the various items as they provide an overall indicator of the pavement performance across the 50-foot long test item. These profiles eliminate some of the discontinuities associated with discrete rutting measurements that may correspond to the weakest, or strongest, station along the pavement section. The pavement profile values do not represent the same measurement as the rut depth, rather representing the permanent deformation of the centerline relative to the initial conditions prior to the onset of traffic testing. Thus, the upheaval is not included in these depths. Figures 24, 25, and 26 show the centerline profiles for Items 1, 4, and 5, respectively, at selected intervals. All three figures show that deformations began to increase rapidly at one or more locations in each test item. These locations correspond to the weakest points in the pavement system. Pavement failure propagates outward from these initial locations, inducing failure in the adjacent areas at an accelerated rate. This type of behavior is typical for traffic testing of thin asphalt pavements, yet the effect becomes more pronounced in accelerated pavement testing due to the hydraulic control of the HVS-A load carriage. During traffic testing, the load cells will measure a sharp decrease in load as the carriage moves over the weak point. The HVS then attempts to compensate for the loss of load, leading to slight overloading of the pavement adjacent to the weak point.

Table 7 summarizes the traffic levels at which the permanent surface deformations along the centerline profile exceeded a number of thresholds along 50% of the test item.

Surface profiles were collected at one foot intervals, providing a better measure of the linear variability of rutting and the rate of failure propagation from weak locations across the test item. However, as noted previously, this method does not incorporate the upheaval used in measuring rut depth. These results follow the same trend as the rut depths in terms of ranking the various treatments based on the sustained traffic.

Table 6. Summary of sustained traffic levels for selected rut depths along 50% of the test item

Test Item	Treatment	0.25 in.	0.50 in.	0.75 in.	1.0 in.
Item 1	TX 140	24,360	100,000+	100,000+	100,000+
Item 4	Control	1,200	5,400	11,780	19,500
Item 5	3 in. AC	4,060	12,640	19,140	26,800

Table 7. Summary of sustained traffic levels for selected permanent deformations along 50% of the test item.

Test Item	Treatment	0.25 in.	0.50 in.	0.75 in.	1.0 in.
Item 1	TX 140	44,600	100,000+	100,000+	100,000+
Item 4	Control	3,290	9,200	20,193	24,282+
Item 5	3 in. AC	7,170	15,700	25,200	33,000

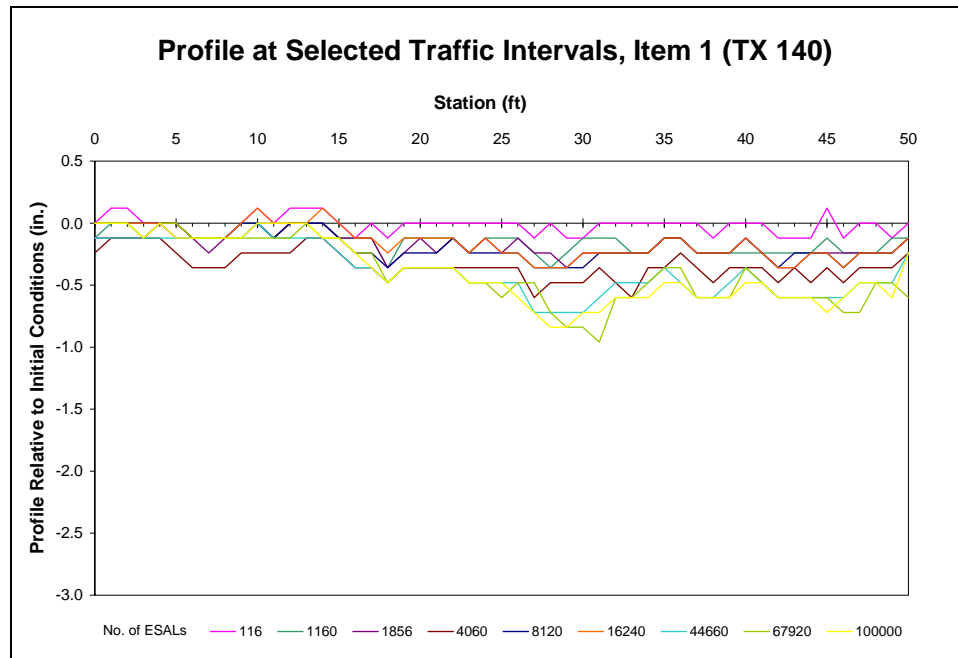


Figure 24. Centerline profiles at selected traffic intervals, Item 1 (TX 140)

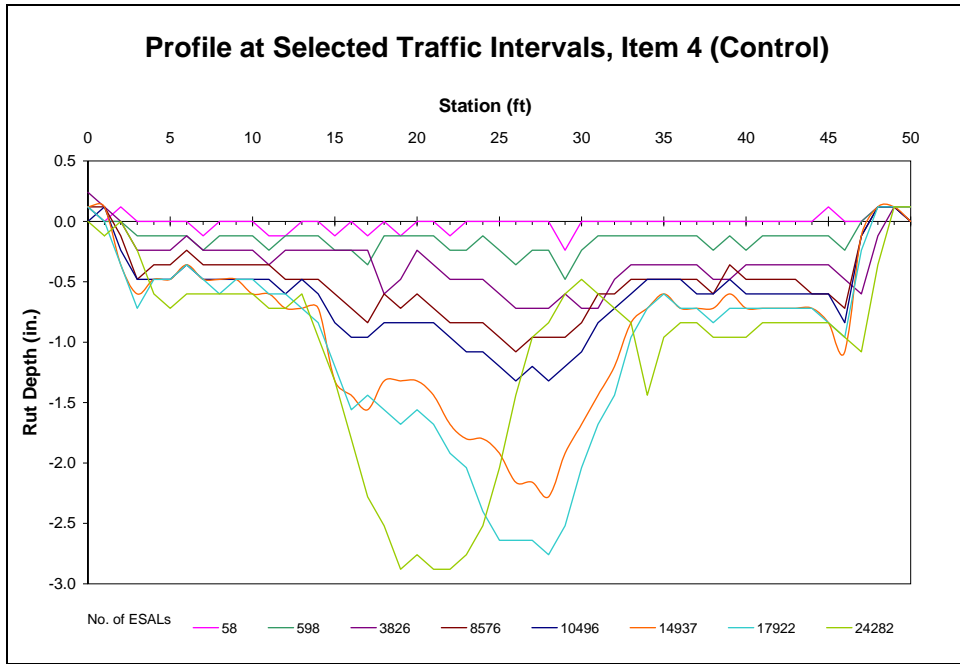


Figure 25. Centerline profiles at selected traffic intervals, Item 4 (Control)

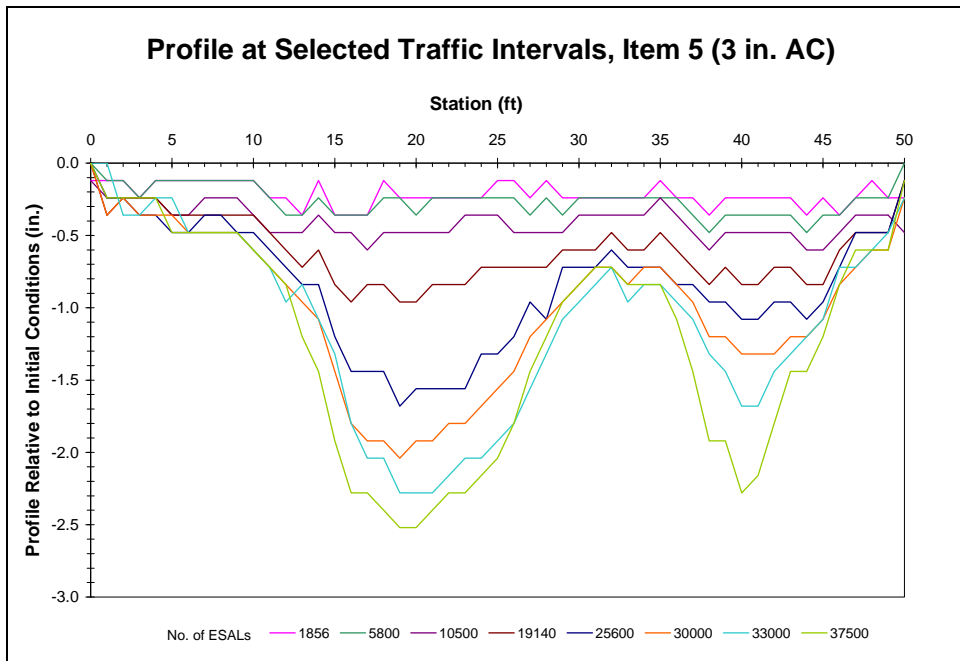


Figure 26. Centerline profiles at selected traffic intervals, Item 5 (3 in. AC).

Pavement Strength

Post-test forensics for Items 1, 4, and 5 included excavation of in-field CBR pits. The asphalt concrete was removed in a 3 ft-long section at Stations 12 and 30. Testing at the base course surface included in-field CBR, DCP, density, and moisture tests. The granular base and geogrid were excavated. Surface testing at the top of the subgrade included CBR, DCP, density, moisture content, and vane shear tests. The results of these tests are summarized in Tables 8-10.

In general, there was not a significant increase in the density of the subgrade. The variability between dry density measurements obtained pre-traffic and during forensics did not present any discernable trends. In general, the density of the base course materials reduced from the levels measured prior to the onset of traffic. This was particularly prominent in those areas where shear flow had initiated. Likewise, base course strengths in the shoulder were reduced from those measured during construction in areas where shear flow had initiated.

Rutting results at these stations were significantly different. Stations at the south end of the test item (Stations 0-15) exhibited significantly less rutting than at the north end of the test item. This is evident at the asphalt surface as well as in the base and subgrade material properties, as shown in Photos 8-13. Photo 11 shows significant rutting in the base course of Item 4 (Control). The base thickness is reduced directly beneath centerline of the traffic line while there is excessive aggregate material in the upheaval area, evidence of shear flow in the base. Photos 12 and 13 show evidence of more moderate shear flow in Item 5 (3 in. AC). Rutting in the base course was not observed in the geogrid reinforced test item (Item 1). As noted previously, trafficking of Item 1 was halted after 100,000 ESALs due to material contamination. The absence of measurable rutting in the base or subgrade may be a result of halting traffic prior to exceeding the 1-in. failure criteria along 50% of the length of the test item.

Table 8. Summary of data collected post-traffic, Item 1

	Wheelpath			Shoulder		
	CBR (%)	Dry Density (pcf)	Moisture Content (%)	CBR (%)	Dry Density (pcf)	Moisture Content (%)
Base						
Station 12	74.9	137.7	2.6	73.4	141.8	2.5
Station 30	100+	145.3	3.1	100+	144.6	3.3
Subgrade						
Station 12	2.1	84.4	35.6	2.2	80.8	37.3

Station 30	2.5	84.1	35.4	2.0	84.7	34.2
------------	-----	------	------	-----	------	------

Table 9. Summary of data collected post-traffic, Item 4

	Wheelpath			Shoulder		
	CBR (%)	Dry Density (pcf)	Moisture Content (%)	CBR (%)	Dry Density (pcf)	Moisture Content (%)
Base						
Station 12	93	146.8	3.1	65	143.5	3.2
Station 30	100+	152.4	2.8	47	146.0	3.0
Subgrade						
Station 12	3.0	85.8	33.3	2.1	84.2	34.9
Station 30	2.5	79.1	41.4	2.0	79.7	39.5

Table 10. Summary of data collected post-traffic, Item 5

	Wheelpath			Shoulder		
	CBR (%)	Dry Density (pcf)	Moisture Content (%)	CBR (%)	Dry Density (pcf)	Moisture Content (%)
Base						
Station 12	100+	150.0	3.0	70	139.2	3.9
Station 30	100+	150.1	2.9	53	143.7	3.5
Subgrade						
Station 12	3.4	82.5	39.7	3.4	78.3	40.9
Station 30	3.5	85.1	34.1	2.6	84.6	34.9



Photo 8. CBR Test Pit, Item 1 (Station 12)



Photo 9. CBR Test Pit, Item 1 (Station 30)



Photo 10. CBR Test Pit, Item 4 (Station 12)



Photo 11. CBR Test Pit, Item 4 (Station 30)



Photo 12. CBR Test Pit, Item 5 (Station 12)



Photo 13. CBR Test Pit, Item 5 (Station 30)

Stiffness

The stiffness of the pavement system was characterized through interpretation of the FWD results. Data were analyzed in terms of the Impulse Stiffness Modulus (ISM), a normalization of the applied load by the resulting deflection at the load plate. This is

considered a representative value for the pavement stiffness. All tests were performed at a temperature of 77°F +/-2°F, reducing the effect of the temperature on the measured stiffness values on the asphalt surface. Figures 27-29 show the degradation of the pavement stiffness under the increasing traffic loads. Each figure contains FWD results from seven locations, Stations 12.5, 17, 21, 25, 29, 33, and 37.5 at selected traffic intervals.

In pavement analysis an ISM of 400 kips/in. is considered a weak pavement (Bush 1986). The measured stiffness values throughout testing remained in this weak pavement condition for all stations tested. This is predominantly a function of the weak subgrade used in the pavement design for this experiment.

At the onset of testing, ISM values were between 100 and 200 kips/in. for the control item (Item 4), and between 200 and 250 kips/in. for 3 in.-thick asphalt item (Item 5). Under sustained traffic loading values dropped to 50 kips/in for Item 4 and Item 5. The drop in stiffness between 2,000 and 10,000 ESALs corresponds to the onset of significant rutting at a traffic level of approximately 5,000 ESALs for Item 4. A similar loss of stiffness was observed during trafficking of Item 5, the thickened asphalt section, at a traffic level of 13,000 ESALs.

Compared to Items 4 and 5, Item 1 exhibited a significantly higher initial stiffness value, approximately 300 kips/in. around station 12 prior to trafficking. The remaining ISM values were between 200 and 250 kips/in. It is important to note that unlike the unreinforced test items, the reduction in stiffness of Item 1 was significantly less than for the unreinforced sections. Under sustained traffic beyond 100,000 ESALs the stiffness values would eventually drop to these levels. This is evidence that the geogrid reinforcement not only provided enhanced stiffness to the aggregate base during construction, it also maintained the stiffness of the aggregate base throughout trafficking to the levels tested in this study.

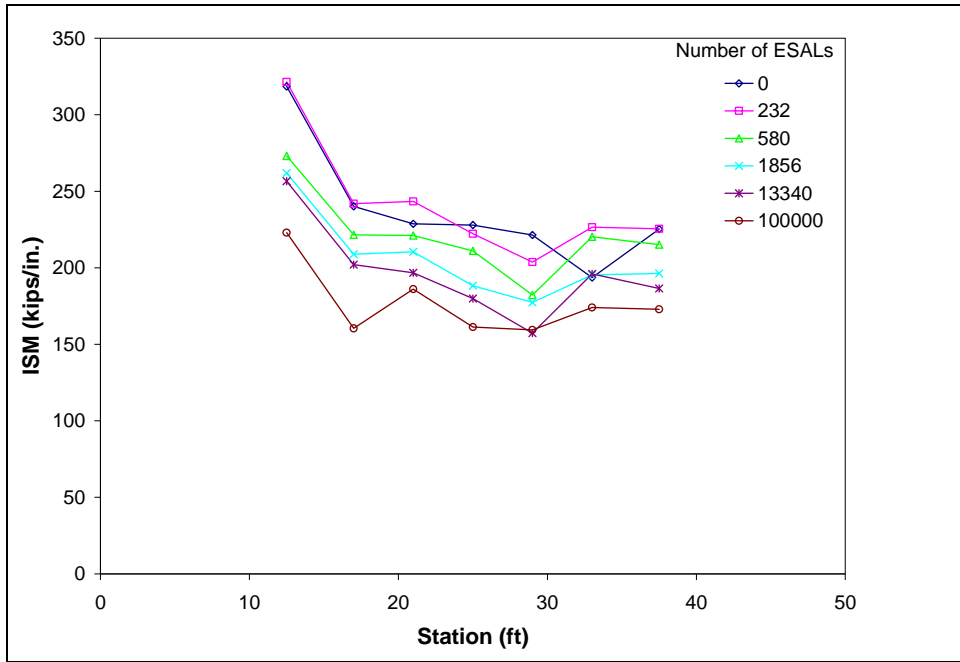


Figure 27. FWD Results at selected traffic intervals, Item 1 (TX 140).

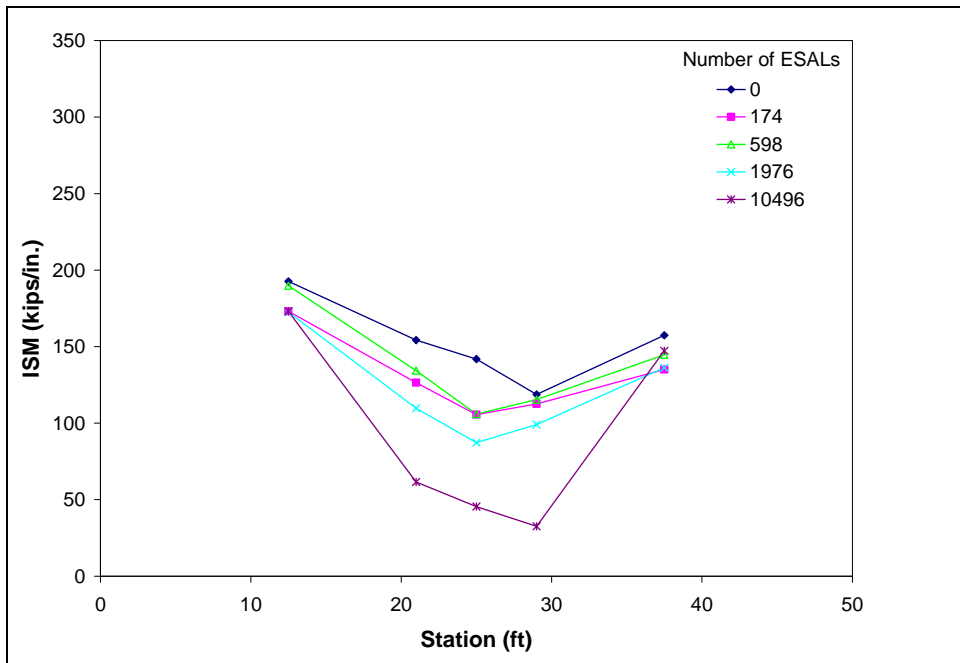


Figure 28. FWD Results at selected traffic intervals, Item 4 (Control).

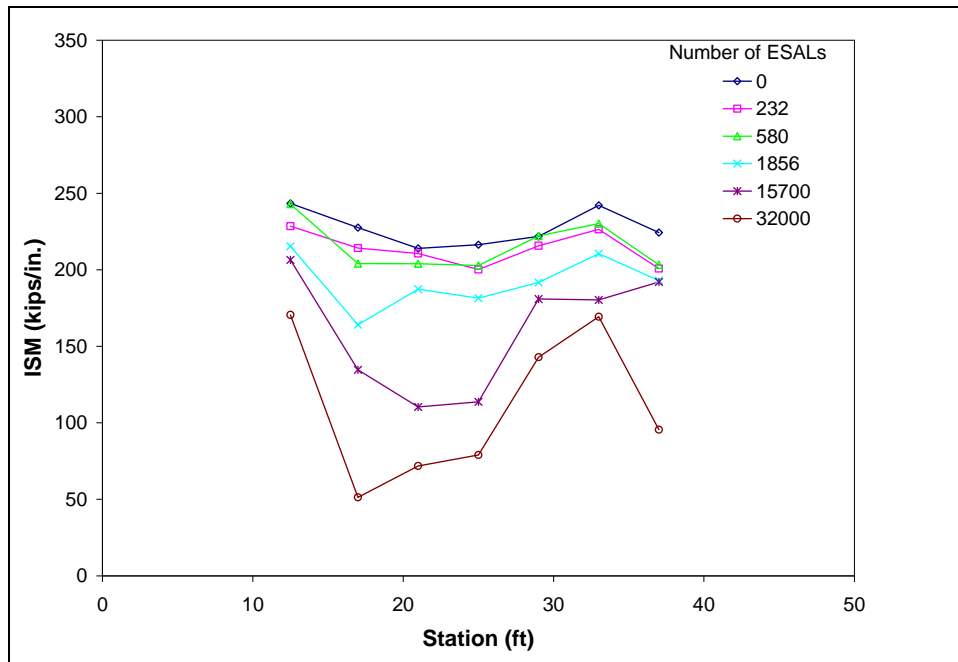


Figure 29. FWD Results at selected traffic intervals, Item 5 (3-in. AC).

Traffic Benefit Ratio

The traditional method of quantifying the relative benefit of a geogrid within the pavement structure is the Traffic Benefit Ratio (TBR). This quantity provides an index of the performance benefit of the geogrid relative to an unreinforced structure. It has been used to quantify and compare life-cycle costs in a cost-benefit analysis. The TBR values measured during this study are summarized in Table 11. The TBR values measured during this study were in excess of 5 for the TX140 product relative to the Control item constructed with a 2-in. thick asphalt concrete surface. It is important to note that TBR values from this study should not be applied in design as direct multipliers to unreinforced design unless the pavement structure, materials and subgrade conditions are essentially identical to those tested in this study. Further, excessive TBR values, such as those observed with TX140 at rut depths less than 0.75 in, should not be interpreted as evidence that the reinforced pavement will have an infinite lifespan. Many factors such as layer thicknesses, base course quality, and subgrade strength will influence the performance benefit provided by a geogrid reinforcement. Therefore, results from experiments like this must be properly interpreted and properly incorporated into design methodologies to insure that the desired reinforced pavement performance results are achieved. Results of experiments such as this are most appropriate to provide a means of validating the performance predicted by design approaches that have incorporated the benefit of geogrid reinforcement.

Table 11. Summary of Traffic Benefit Ratios at various rut depths relative to 2 in. AC Control

Test Item	Treatment	0.25 in.	0.50 in.	0.75 in.	1.0 in.
Item 1	TX 140	20	19+	8+	5+
Item 4	Control	--	--	--	--
Item 5	3 in. AC	3	2	2	1

References

- American Associate for State Highway and Transportation Officials (AASHTO). 1993. *Guide for Design of Pavement Structures*, Washington D.C.
- _____. 2004. *Standard Method of Test for Resistance to Plastic Flow of Bituminous Mixtures Using Marshall Apparatus*, AASHTO T245-97, Washington, D.C.
- _____. 2006. *Standard Method of Test for Sieve Analysis of Fine and Coarse Aggregates*, AASHTO T027-06, Washington, D.C.
- _____. 2007. *Standard Method of Test for Percent Air Voids in Compacted Dense and Open Asphalt Mixtures*, AASHTO T269-97, Washington, D.C.
- _____. 2008. *Standard Method of Test for Theoretical Maximum Specific Gravity and Density of Hot Mix Asphalt (HMA)*, AASHTO T209-08, Washington, D.C.
- American Society for Testing and Materials (ASTM). 2004. *Standard test method for CBR (California Bearing Ratio) of soils in place*. Designation: D 4429-04. West Conshohocken, PA
- _____. 2002. *Standard test methods for laboratory compaction characteristics of soil using modified effort*. Designation: D 1557-07. West Conshohocken, PA
- _____. 2004. *Standard test methods for liquid limit, plastic limit, and plasticity index of soils*. Designation: C 856-02-07. West Conshohocken, PA
- _____. 2004. *Standard test methods for water content of soil and rock in place by nuclear methods (shallow depth)*. Designation: D 3017-04. West Conshohocken, PA
- _____. 2004. *Standard test methods for classification of soils for engineering purposes (Unified Soil Classification System)*. Designation: D 2487-06. West Conshohocken, PA
- _____. 2009. *Standard Test Method for Use of the Dynamic Cone Penetrometer in Shallow Pavement Applications*. Designation: D 6951-09. West Conshohocken, PA
- Bush III, A.J.. 1986. *Performance Prediction of Low Volume Airfield Pavements*. TR GL-86-14. Vicksburg, MS: U. S. Army Waterways Experiment Station.
- Headquarters, Department of the Army. 1992. *Pavement Design for Roads, Streets, Walkways, and Open Storage Areas*, Technical Manual TM 822-5-5, Washington, D.C.
- Huang, Y.H. 2004. *Pavement Analysis and Design*, 2nd Edition, Prentice Hall, Upper Saddle River, NJ.

Timm, D.H., and A. L. Priest. 2005. Wheel Wander at the NCAT Test Track, NCAT Report 05-02. Auburn, AL.

Webster, S.L., R.H. Grau, and T.P. Williams. 1992. *Description and application of dual-mass dynamic cone penetrometer*. Instruction Report GL-92-3. Vicksburg, MS: US Army Engineer Waterways Experiment Station.

Webster, S.L., R.W. Brown, and J.R. Porter. 1994. *Force projection site evaluation using the electrical cone penetrometer (ECP) and the dynamic cone penetrometer (DCP)*. Technical Report GL-94-17. Vicksburg, MS. U.S. Army Waterways Experiment Station